



1 **Trends and spatial shifts in lightning fires and smoke concentrations**
2 **in response to 21st century climate over the forests of the Western**
3 **United States**

4 Yang Li¹, Loretta J. Mickley¹, Pengfei Liu¹, and Jed O. Kaplan²

5 ¹John A. Paulson School of Engineering and Applied Sciences, Harvard University, Cambridge,
6 MA, USA

7 ²Department of Earth Sciences, The University of Hong Kong, Hong Kong, China

8 *Correspondence to:* Yang Li (yangli@seas.harvard.edu)

9

10 **Abstract.** Almost US\$ 3bn per year is appropriated for wildfire management on public land in the
11 United States. Recent studies have suggested that ongoing climate change will lead to warmer and
12 drier conditions in the Western United States with a consequent increase in the number and size of
13 wildfires, yet large uncertainty exists in these projections. To assess the influence of future changes
14 in climate and land cover on lightning-caused wildfires in National Forests and Parks of the
15 Western United States and the consequences of these fires on air quality, we link a dynamic
16 vegetation model that includes a process-based representation of fire (LPJ-LMfire) to a global
17 chemical transport model (GEOS-Chem). Under a scenario of moderate future climate change
18 (RCP4.5), increasing lightning-caused wildfire enhances the burden of smoke fine particulate
19 matter (PM), with mass concentration increases of ~53% by the late-21st century during the fire
20 season. In a high-emissions scenario (RCP8.5), smoke PM concentrations double by 2100. RCP8.5
21 also shows large, northward shifts in dry matter burned, leading to enhanced lightning-caused fire
22 activity especially over forests in the northern states.



23 1 Introduction

24 Both the incidence and duration of large wildfires in the forests of the western United States
25 have increased since the mid-1980s (Westerling et al., 2006; Abatzoglou and Williams, 2016),
26 affecting surface levels of particulate matter (Val Martin et al., 2006), with consequences for
27 human health (Liu et al., 2017) and visibility (Spracklen et al., 2009; Ford et al., 2018). Wildfire
28 activity is influenced by a combination of different factors, including fuel load, fire suppression
29 practices, land use, land cover change, and meteorology (Pechony and Shindell, 2010). Over the
30 forests of the Western United States (WUS), lightning-caused wildfires account for the majority
31 of burned area (Abatzoglou et al., 2016) and have driven most of the recent increase in large
32 wildfires, with human ignition contributing less than 12% to this trend (Westerling, 2016). Studies
33 suggest that a warming climate could enhance wildfires in the WUS (Yue et al., 2013; Abatzoglou
34 and Williams, 2016), but quantifying future wildfire activity is challenging, given uncertainties in
35 land cover trends and in the relationships between fire and weather. Not all studies have accounted
36 for changing land cover or have distinguished the effects of lightning fire ignitions from human-
37 started fires. In this study, we project lightning-caused fire emissions over the National Parks and
38 Forests of the WUS in the mid- and late- 21st century, using a dynamic global vegetation model
39 combined with a chemical transport model. Our goal is to understand how trends in both land cover
40 and meteorology may affect natural fire activity and smoke air quality over the 21st century.

41 Consistent with projections of increasing wildfire in the WUS, recent studies have also
42 predicted enhancement of fire-generated PM under a warmer and drier climate in this region (Yue
43 et al., 2013; Yue et al., 2014; Spracklen et al., 2009; Ford et al., 2018; Westerling et al., 2006).
44 Some of these studies relied on statistical models that relate meteorological variables to fire metrics
45 such as area burned; these models can then be applied to projections from climate models (Yue et



46 al., 2013; Yue et al., 2014; Spracklen et al., 2009; Archibald et al., 2009; Wotton et al., 2003;
47 Westerling and Bryant, 2008). However, these statistical methods do not account for changes in
48 vegetation due to climate, increasing atmospheric CO₂ concentrations, or land use. A further
49 weakness of these studies is that they do not consider whether enhanced fire activity in the future
50 atmosphere may ultimately deplete the supply of woody fuels (Yue et al., 2013; Yue et al., 2014).
51 Other studies have coupled global vegetation models to climate models to better represent such
52 fire-vegetation-climate interactions (Chaste et al., 2018). These coupled models integrate
53 vegetation dynamics, land-atmosphere exchanges, and other key physical processes, allowing
54 consideration of many factors driving fire activity and smoke pollution on regional scales (Ford et
55 al., 2018). Building on this research, we use an integrated vegetation-climate model system with
56 these aims: (1) to clarify how changing meteorology and vegetation together drive future lightning-
57 caused wildfire activity and (2) to provide predictions of smoke pollution at finer spatial resolution
58 than previously. Our approach accounts for the impact of future climate and lightning fires on fuel
59 structure, and these fine-scale predictions are of greater utility to environmental managers and
60 especially the health impacts community.

61 Lightning is the predominant cause of wildfire ignition in most mountainous and forest
62 regions of the WUS during months that have high fire frequency (Abatzoglou et al., 2016; Balch
63 et al., 2017). In remote and mountainous terrain, anthropogenic ignitions are infrequent and >90%
64 of total area burned is caused by lightning-started fires (Abatzoglou et al., 2016). Here we study
65 lightning-caused fires over the National Parks and Forests of the WUS in the mid- and late- 21st
66 century under two future climate change scenarios defined by Representative Concentration
67 Pathways (RCPs). RCP4.5 represents a moderate pathway with gradual reduction in greenhouse
68 gas (GHG) emissions after 2050, while RCP8.5 assumes continued increases in GHGs throughout



69 the 21st century. We use the Lund-Potsdam-Jena-Lausanne-Mainz (LPJ-LMfire) Dynamic Global
70 Vegetation Model (Pfeiffer et al., 2013) to simulate dynamic fire-vegetation interactions under
71 future climate. LPJ-LMfire, which has been used previously to investigate historical fire activity
72 (e.g., Chaste et al., 2018), is applied here to estimate natural fire emissions under future climate
73 simulated by the Goddard Institute for Space Studies (GISS) Model E climate model.

74 July, August, and September (JAS) are the months of greatest fire activity in WUS forests
75 (Park et al., 2003) and the focus of our study. We limit the spatial extent of our analyses to the
76 National Parks and Forests of the WUS, here defined as 31°N – 49°N, 100°W – 125°W. For
77 RCP4.5, the GISS model predicts a statistically significant increase in surface temperature of 1.4
78 K averaged over the entire region by 2050 during JAS; for RCP8.5, the mean JAS temperature
79 increase is 3.7 K by 2100. In both future climate scenarios, significant precipitation decreases of
80 ~20% by 2100 are simulated. Several studies have predicted future increases in lightning due to
81 climate change (e.g., Price and Rind, 1994a,). However, the relationship between lightning flash
82 rate and meteorology is poorly constrained in models and depends largely on physical parameters
83 such as cold cloud thickness, cloud top height, or convective available potential energy. In our
84 study, we use the convective mass flux from the GISS model to calculate lightning density in terms
85 of flashes km⁻² day⁻¹. Unlike surface temperature and precipitation, we find that average lightning
86 density over the West does not change significantly during the 21st century, as described in Fig.
87 S1.

88 LPJ-LMfire simulates wildfire emissions of black carbon (BC) and organic carbon (OC)
89 particles, which are then passed to the global atmospheric chemistry-transport model GEOS-Chem,
90 to simulate the transport and distribution of wildfire smoke across the West. For each RCP, LPJ-
91 LMfire simulates vegetation dynamics and fire continuously for the period 2006-2100, with



92 monthly resolution. For reasons of computational demand, we were limited to conducting two
93 time-slice simulations with GEOS-Chem focused around 2010 and 2100, with each time slice
94 covering 5 continuous years. For further details, see Methods section below.

95

96 **2 Methods**

97 We quantify the effects of changing climate on area burned and fire emissions caused by
98 lightning over the National Forests in the WUS using the LPJ-LMfire model (Pfeiffer et al., 2013),
99 driven by meteorological fields from the GISS-E2-R climate model (Nazarenko et al., 2015).
100 Natural wildfire emissions of dry matter burned calculated by LPJ-LMfire are then passed to
101 GEOS-Chem, a 3-D chemical transport model, to simulate the transport of wildfire smoke across
102 the WUS.

103 **2.1 LPJ-LMfire**

104 The LPJ-LMfire dynamic vegetation model is driven by gridded climate, soil, land use
105 fields, and atmospheric CO₂ concentrations, and simulates vegetation structure, biogeochemical
106 cycling, and wildfire (Pfeiffer et al., 2013; Sitch et al., 2003). Wildfires are simulated based on
107 processes including explicit calculation of lightning ignitions, the representation of multi-day
108 burning and coalescence of fires, and the calculation of rates of spread in different vegetation types
109 (Pfeiffer et al., 2013). The climate anomaly fields from the GISS-E2-R climate model used to
110 prepare a future scenario for LPJ-LMfire are monthly mean surface temperature, diurnal
111 temperature range (i.e., the difference between monthly mean daily maximum and daily minimum
112 temperatures), total monthly precipitation, number of days in the month with precipitation greater
113 than 0.1 mm, monthly mean total cloud cover fraction, and monthly mean surface wind speed.
114 This version of the GISS model was configured for Phase 5 of the Coupled Model Intercomparison



115 Project (CMIP5) (Nazarenko et al., 2015). Lightning strike density for application in LPJ-LMfire
116 is calculated using the GISS convective mass flux following the empirical parameterization of
117 Magi, 2015. We run LPJ-LMfire on a $0.5^\circ \times 0.5^\circ$ global grid, though for this study only results over
118 the National Parks and Forests of the WUS are analyzed.

119 The GISS-E2-R meteorology used here covers the period 1801-2100 at a resolution of 2°
120 latitude \times 2.5° longitude. The start year of the two climate scenarios, RCP4.5 and RCP8.5, is 2006.
121 The two RCPs capture a range of possible climate trajectories over the 21st century, with radiative
122 forcings at 2100 relative to pre-industrial values of $+4.5 \text{ W m}^{-2}$ for RCP4.5 and $+8.5 \text{ W m}^{-2}$ for
123 RCP8.5. From 2011 to 2015, the greenhouse gas concentrations of the two scenarios are nearly
124 identical. To downscale the GISS meteorological fields to finer resolution for LPJ-LMfire, we first
125 calculate the 2010-2100 monthly anomalies relative to the average over the 1961-1990 period, and
126 then add the resulting timeseries to a high-resolution observationally based climatology at 0.5°
127 latitude \times 0.5° longitude spatial resolution. The climatology was prepared using the datasets
128 including WorldClim 2.1, Climate WNA, CRU CL 2.0, Wisconsin HIRS Cloud Climatology, and
129 LIS/OTD, as described in Pfeiffer et al., 2013. The LPJ-LMfire simulations used here cover the
130 period 2006-2100 at a monthly timestep. Future land use scenarios applied follow those in CMIP5,
131 in which the extent of crop and pasture cover in the WUS increases by 30% in future climates
132 (Brovkin et al., 2013; Kumar et al., 2013).

133 Passive fire suppression results from landscape fragmentation caused by land use (e.g., for
134 crop and grazing land, roads, and urban areas), and this influence on fire activity is included in the
135 LPJ-LMfire simulations (Pfeiffer et al., 2013). The model does not, however, consider the active
136 fire suppression practiced throughout much of the WUS. We therefore limit our study to wildfire
137 activity on the National Park and Forest lands of the WUS that are dominated by lightning fires



138 and where land use for agriculture and urban areas is minimal. To focus only on National Park and
139 Forest lands, we apply a $0.5^\circ \times 0.5^\circ$ raster across the WUS that identifies the fraction of each grid
140 cell that belongs to a National Forest or National Park, and we consider only these areas in our
141 analysis.

142 **2.2 Fire emissions**

143 Fuel biomass in LPJ-LMfire is discretized by plant functional type (PFT) into specific live
144 biomass and litter categories, and across four size classes for dead fuels. The model simulates
145 monthly values of total dry matter burned for nine PFTs as in Pfeiffer et al., 2013. To pass LPJ-
146 LMfire biomass burning emissions to GEOS-Chem, we first reclassify these nine PFTs into the
147 six land cover types considered by GEOS-Chem. See Table 2 for a summary of the reclassification
148 scheme. Tropical broadleaf evergreen, tropical broadleaf raingreen, and C_4 grasses are not
149 simulated by LPJ-LMfire in the National Parks and Forests of the WUS. Emission factors based
150 on the six land cover types in GEOS-Chem are then applied to dry matter burned from LPJ-LMfire,
151 resulting in monthly BC and OC emissions over National Forests. These factors are from Akagi et
152 al., 2011. As lightning-started wildfires are dominant over the WUS forests, an evaluation of fire
153 emissions over National Park and Forest lands from the LPJ-LMfire model against the Global Fire
154 Emissions Database (GFED4s) inventory (Giglio et al., 2013) is included in the Supplement (Fig.
155 S2).

156 **2.3 GEOS-Chem**

157 We use the GEOS-Chem chemical transport model (version 12.0.1;
158 <http://acmg.seas.harvard.edu/geos/>). For three time slices including the present day, mid- and late-
159 21st century, we compare the five-year averaged (i.e., 2011-2015, 2051-2055, 2096-2100) living
160 biomass and lightning fire emissions from the continuous LPJ-LM simulations with ten-year



161 averages (i.e., 2006-2015, 2046-2055, 2091-2100). We find differences of less than 20% caused
162 by extending the length of the time slices. We therefore perform two five-year time slice
163 simulations for each RCP, covering the present day (2011-2015) and the late-21st century (2096-
164 2100). For each time slice, we first carry out a global simulation at 4° latitude x 5° longitude spatial
165 resolution, and then downscale to 0.5° × 0.625° over the WUS via grid nesting over the North
166 America domain. For computational efficiency, we use the aerosol-only version of GEOS-Chem,
167 with monthly mean oxidants archived from a full-chemistry simulation, as described in Park et al.,
168 2004. The GEOS-Chem simulations are driven with present-day MERRA-2 reanalysis
169 meteorology from NASA/GMAO (Gelaro et al., 2017) to isolate the effect of changing wildfires
170 on U.S. air quality. The simulations include emissions of all primary PM and the gas-phase
171 precursors to secondary particles, with non-fire particle sources comprising fossil fuel combustion
172 from transportation, industry, and power plants from the 2011 EPA NEI inventory. In the future
173 time slices, non-fire emissions remain fixed at present-day levels.

174 Our study focuses on carbonaceous PM (smoke PM; BC+OC), which are the main
175 components in wildfire smoke (Chow et al., 2011). For the present day, we apply 5-year (2011-
176 2015) averaged GFED4s emissions to those regions that fall outside National Forests and
177 temporally changing LPJ-LMfire emissions from the two RCPs within the Forests (Figs. S3-S4).
178 Implementing the combined emissions allow us to further validate the simulated results in this
179 study using observations. For the future time slices, we assume that fires outside the National
180 Forests remain at present-day levels, and we again combine the 2011-2015 GFED4s fire emissions
181 with the temporally changing, future LPJ-LMfire emissions over the National Forests.

182

183



184 3 Results

185 3.1 Spatial shifts in fire activity

186 Under both RCPs, 21st century climate change and increasing atmospheric CO₂
187 concentrations lead to shifts in the distribution of total living biomass and dry matter burned. Fig.
188 1 shows the changes in monthly mean temperature and precipitation averaged zonally over grid
189 cells at each 1° latitude of the West, relative to the present day, defined as ~2010. Peak temperature
190 enhancements in JAS occur between 36°-42° N for ~2050 and ~2100 in both RCPs, with a
191 maximum enhancement of 4 °C for RCP4.5 and 6 °C for RCP8.5 in 2100. Significant decreases
192 in JAS precipitation occur between 33°-45° N under RCP4.5 and at latitudes north of 39° N under
193 RCP8.5 for ~2100. The maximum decrease in monthly precipitation over the West is ~40 kg m⁻²
194 (~60%) in JAS under both RCPs. These warmer and drier conditions favor fire activity under future
195 climate.

196 Fires and smoke production are dependent on fuel load, and throughout the 21st century,
197 total living biomass in the WUS is primarily concentrated in northern forests (Fig. 2). For RCP4.5,
198 living biomass exhibits significant enhancements in U.S. National Parks and Forests at latitudes
199 north of 43° N in the 2050 time slice and north of 45° N in the 2100 time slice. North of 46° N,
200 the change in living biomass at 2100 (~0.4 kg C m⁻²) is double that at 2050 (~0.2 kg C m⁻²). At
201 latitudes south of 40°N, living biomass in RCP4.5 is generally invariant over the 21st century. In
202 RCP8.5, living biomass also increases significantly near the Canadian border – e.g., as much as
203 ~0.2 kg C m⁻² for the 2050 time slice and ~0.4 kg C m⁻² for the 2100 time slice, relative to the
204 present day. In contrast, at latitudes between 42°-47° N in RCP8.5, total living biomass decreases
205 by as much as -0.6 kg C m⁻² for ~2100. For both RCPs, these mid-century and late-century changes
206 in total living biomass are significant ($p < 0.05$) across nearly all latitudes. In RCP4.5, the spatial



207 shifts of total living biomass are relatively weak from 2050 to 2100, consistent with the moderate
208 climate scenario with gradual reduction in greenhouse gas emissions after 2050. However, under
209 the continued-emissions climate scenario RCP8.5, total living biomass in these forests first
210 increases by 2050 and then decreases by ~10% by 2100, indicating a strongly disturbed vegetation
211 system due to climate change. Despite this decrease, living biomass in this scenario is still
212 abundant in the West in 2100, especially over the northern forests (not shown), suggesting that
213 future climate change will not limit fuel load. Table 1 summarizes these results.

214 LPJ-LMfire simulates boreal needleleaf evergreen and boreal and temperate summergreen
215 (broadleaf) trees as the dominant plant functional types (PFTs) in the National Parks and Forests
216 of the WUS; these PFTs together account for ~90% of the total biomass in our study domain.
217 Changes over the 21st century (Fig. 2) reflect the changes in the growth and distribution of these
218 PFTs, with increases in living biomass in the north and decreases in the south in both RCP
219 scenarios (Fig. S5). In the 2100 time slice, vegetation shifts further north than in the 2050 time
220 slice. The reasons for this shift can be traced to the climate regimes favored by different vegetation
221 types, with temperate and boreal trees showing moderate to strong inclination in their growth along
222 the north-south temperature gradient (Aitken et al., 2008). For example, the temperate broadleaf
223 summergreen PFT favors regions with moderate mean annual temperatures and distinct warm and
224 cool seasons (Jarvis and Leverenz, 1983), while boreal needleleaf evergreen generally occurs in
225 colder climate regimes (Aerts, 1995). With rising temperatures, the living biomass of temperate
226 summergreen trees increases in most states in the WUS, with maximum enhancement of +1.0 kg
227 C m⁻² in western Washington, northern Montana, and Idaho by 2100 in RCP8.5 relative to 2010.
228 Decreases in this vegetation type for this scenario occur in the south, as much as -0.5 kg C m⁻² in
229 New Mexico. In contrast, boreal trees increase in only a few regions in the far north, with a



230 substantial contraction in their abundance over much of the West, as much as -4.0 kg C m^{-2} for
231 boreal needleleaf evergreen by 2100 in RCP8.5 over the northern forests.

232 Simulated area burned from lightning-ignited fires in the National Parks and Forests of the
233 WUS increases by $\sim 30\%$ by ~ 2050 , and by $\sim 50\%$ by ~ 2100 for both RCPs (not shown),
234 comparable to the predicted 78% increase in lightning-caused area burned in the U.S. under a
235 doubled CO_2 climate by Price and Rind, 1994b. That study, however, projected an increase in
236 lightning flashes and did not consider changing land cover. The changes we calculate at 2050 are
237 also within the range of previous studies using statistical methods for this region (e.g., 54% in
238 Spracklen et al., 2009 and 10-50% in Yue et al., 2013). Fig. 2 further shows that dry matter burned,
239 a function of both area burned and fuel load, increases relative to the present at most latitudes at
240 both 2050 and 2100 and in both RCPs. Year-to-year variations in dry matter burned are greater
241 than those in living biomass due to variations in the meteorological conditions driving fire
242 occurrence. Previous studies have found that interannual variability in wildfire activity is strongly
243 associated with regional surface temperature (Westerling et al., 2006; Yue et al., 2013). We show
244 here that although total living biomass mostly decreases at latitudes $\sim 45^\circ \text{ N}$ by ~ 2100 under
245 RCP8.5, the peak enhancements in dry matter burned also occur at these latitudes, indicating that
246 the modeled changes in fire activity are driven by changes in meteorological conditions that favor
247 fire, as well as by shifts towards more pyrophilic landscapes such as open woodlands and savannas.
248 As with biomass, lightning-caused fires also shift northward over the 21st century, especially in
249 RCP8.5. In this scenario, dry matter burned increases by as much as $35 \text{ g m}^{-2} \text{ mon}^{-1}$ across 40° -
250 48° N at ~ 2100 compared to the present day. By 2100, the fire-season total dry matter burned over
251 the forests in the West increases by 24.58 Tg/JAS (111%) under RCP4.5 and by 50.00 Tg/JAS
252 (161%) in RCP8.5 (Table 1).



253 The spatial distributions of changes in total living biomass and dry matter burned are shown
254 in Fig. 3. Under RCP4.5, moderate decreases in total living biomass (by as much as -2.5 kg C m^{-2})
255 and increases in dry matter burned by 2100 (up to $\sim 70 \text{ g m}^{-2} \text{ mon}^{-1}$) are concentrated in central
256 Idaho, Wyoming, and Colorado. Large declines in total living biomass and enhancements in dry
257 matter burned occur in the forests of Idaho and Montana by 2100 under RCP8.5, with a hotspot of
258 -5.0 kg C m^{-2} in biomass and $+100 \text{ g m}^{-2} \text{ mon}^{-1}$ in dry matter burned in Yellowstone National Park.
259 Similar trends in total living biomass and dry matter burned are also predicted for the Sierra
260 Nevada (SN) region in California (Fig. S6). As shown in Table 1, predicted changes in dry matter
261 burned over the SN forests by 2050 are 17-44%, comparable to the calculated future increases of
262 30-50% by Yue et al., 2014. We find significant increases in dry matter burned of 81% by 2100
263 under RCP8.5 in this region. Our results suggest that even as future climate change diminishes
264 vegetation biomass in some regions of the WUS, sufficient fuel still exists to allow increases in
265 fire activity and dry matter burned.

266 **3.2 Smoke PM**

267 Given the large uncertainty in secondary aerosol formation within smoke plumes (Ortega
268 et al., 2013), we assume that smoke PM mainly consists of primary BC and OC. We calculate
269 emissions of fire-specific BC and OC by combining the estimates of the dry matter burned with
270 emissions factors from Akagi et al., 2011, which are dependent on land cover type. Application of
271 these emissions to GEOS-Chem allows us to simulate the transport and distribution of smoke PM
272 across the WUS.

273 With increasing lightning fire activity in most of the National Park and Forest areas of the
274 WUS over the 21st century (Fig. 3), smoke PM shows modest enhancement for RCP4.5, but more
275 substantial increases for RCP8.5 (Fig. 4). Smoke PM enhancements in RCP4.5 occur primarily



276 over the forests along the state boundaries of Idaho, Montana, and Wyoming, with large increases
277 by as much as $\sim 10 \mu\text{g m}^{-3}$ in Yellowstone National Park. Scattered increases in smoke PM in
278 RCP4.5 are also predicted over the forests in northern Colorado, northern California, western
279 Oregon, and central Arizona. In RCP8.5, smoke PM enhancements are widespread over the
280 northern states of the WUS by 2100, with significant increases in regions east of the Rocky
281 Mountains. Increased fire activity and large smoke PM enhancements are seen by 2100 in RCP8.5,
282 including large areas of the Flathead, Nez Perce, Clearwater, Arapaho, and Roosevelt National
283 Forests. Particularly large increases – as much as $\sim 40 \mu\text{g m}^{-3}$ – occur in Yellowstone National Park.
284 The increases in fire in these forests significantly influences air quality over the entire area of
285 Idaho, Montana, Wyoming, and Colorado, with effects extending eastward to Nebraska and the
286 Dakotas. Increased smoke PM is also predicted over the Sierra Nevada in both RCPs. In RCP4.5,
287 average smoke PM over the entire WUS increases by 53% compared to present (Table 1). For
288 RCP8.5, smoke PM more than doubles (109% increase) at ~ 2100 .

289

290 **4 Discussion**

291 We apply a coupled modeling approach to investigate the impact of changes in climate and
292 vegetation on future lightning-caused wildfires and smoke pollution across the WUS in the 21st
293 century. For RCP4.5, the late-21st century lightning-caused wildfire-specific smoke PM in the
294 West increases $\sim 53\%$ relative to present. Comparable fire activity between 2050 and 2100 reflect
295 the effectiveness of the emission reduction strategies after 2050 under RCP4.5, as temperature
296 changes across the West are relatively flat from 2050 to 2100, with a nearly constant area-averaged
297 mean annual temperature of $\sim 19.2^\circ\text{C}$. In RCP8.5, mean annual temperatures continue increasing
298 over the second half of the 21st century across the West, nearly 2.1°C from 2050, and wildfire-



299 specific PM concentrations double by 2100.

300 In table S1 we compare predictions in this study with previous fire estimates under future
301 climate. A difference between these studies and ours is that we consider only changes in fire
302 activity over the National Parks and Forests while others examine changes over the whole WUS.
303 However, we find that in the GFED4s inventory, present-day fire emissions outside these federally
304 managed areas contribute less than 1% of DM burned. Also, the fact that lightning is the dominant
305 driver of wildfire activity over the WUS forests (Balch et al., 2017) allows a reasonable
306 comparison of the estimates in this study with those in previous studies that include both lightning
307 and human-started fires over the West.

308 Table S1 shows that fire activity in the U.S. is predicted to increase in all studies cited.
309 However, the projected changes in fire metrics such as area burned or in emissions or
310 concentrations of smoke vary greatly across studies, from ~10-300% relative to present-day values.
311 These discrepancies arise from differences in the methodologies, fire assumptions, and future
312 scenarios applied. The ~80% increases in smoke emissions that we project by 2050 is generally
313 lower than estimates in previous statistical studies (e.g., 150-170% in Yue et al., 2013 or 100% in
314 Spracklen et al., 2009), but comparable to the predicted 78% increase in lightning-caused area
315 burned in the U.S. under a doubled CO₂ climate by Price and Rind, 1994b, which did not account
316 for vegetation changes due to climate change or changing CO₂. In contrast, the ~80% increase in
317 smoke emissions in this study at ~2050 are substantially higher than the ~40% increases predicted
318 by Ford et al., 2018 over the West, though the magnitudes of emission changes in the two studies
319 are similar. As in our study, Ford et al., 2018 relied on a land cover model, but they also attempted
320 to account for the influence of future changes in meteorology and population on the suppression
321 and ignition of fires. Ford et al., 2018 predicted scattered emission increases of 40-45% over the



322 West and a large increase of 85-220% over the Southeast due to increasing population and the role
323 of human ignition. However, human activities have diverse impacts on wildfires, and those impacts
324 are a function of land management policy, economics, and other social trends, making it
325 challenging to predict how trends in human ignitions, fuel treatment, and fire suppression will
326 evolve in the future (Fusco et al., 2016). In our study, we confine our focus to fires in National
327 Parks and Forests in the West, where human activities such as landscape fragmentation through
328 land use are less important. We further find that the patterns of increasing fire emissions by 2100
329 in our study – i.e., over the forests in northern Idaho, western Montana, and over the U.S. Pacific
330 Northwest – are similar to those predicted by other studies, including Rogers et al., 2011 and Ford
331 et al., 2018. Our study also predicts significantly elevated smoke PM in Utah, Wyoming, and
332 Colorado in the late-21st century under RCP8.5 and in regions east of the Rocky Mountains because
333 of the prevailing westerly winds.

334 The following limitations apply to our study. The vegetation model simulations of biomass
335 and fire are driven by meteorology from just one climate model, GISS-E2-R. Over the WUS, this
336 model simulates future temperature changes at the low end of projections by the CMIP5 ensemble,
337 making our predictions of future fire conservative (Sheffield et al., 2013; Ahlström et al., 2012;
338 Rupp et al., 2013). Anthropogenic ignitions are not considered in this study, but fire behavior and
339 therefore burned area are primarily governed by meteorology and fuel structure, both of which are
340 simulated by LPJ-LMfire. The fire simulations are performed on a $0.5^\circ \times 0.5^\circ$ grid, which cannot
341 capture some the fine-grain structure of the complex topography and sharp ecotones present in our
342 study area (e.g., Shafer et al., 2015). Our study also does not consider the effects of future climate
343 change on the transport or lifetime of smoke PM. Previous work, however, has shown that such
344 effects on smoke PM are likely to be small relative to the effect of changing wildfire activity



345 (Spracklen et al., 2009).

346 Within these limitations, our results highlight the vulnerability of the WUS to lightning-
347 caused wildfire in a changing climate. Even though a changing climate decreases the living
348 biomass in some regions, we find that ample vegetation exists to fuel increases in fire activity and
349 smoke. Especially strong enhancements in smoke PM occur in the Northern Rockies in the late-
350 21st century under both the moderate and strong future emissions scenarios, suggesting that climate
351 change will have a large, detrimental impact on air quality, visibility, and human health in a region
352 valued for its National Forests and Parks. Our study thus provides a resource for environmental
353 managers to better prepare for air quality challenges under a future climate change regime.

354

355

356

357 **Data availability**

358 Data related to this paper may be requested from the authors.

359

360 **Author contributions**

361 Y.L. conceived and designed the study, performed the GEOS-Chem simulations, analyzed the data,
362 and wrote the manuscript, with contributions from all coauthors. J.O.K. performed the LPJ-LMfire
363 simulations.

364

365 **Competing interests**

366 The authors declare that they have no competing interest.

367



368 **Acknowledgments**

369 This research was developed under Assistance Agreements 83587501 and 83587201 awarded by
370 the U.S. Environmental Protection Agency (EPA). It has not been formally reviewed by the EPA.
371 The views expressed in this document are solely those of the authors and do not necessarily reflect
372 those of the EPA. We thank all of the data providers of the datasets used in this study. PM data
373 was provided by the Interagency Monitoring of Protected Visual Environments (IMPROVE;
374 available online at <http://vista.cira.colostate.edu/improve>). IMPROVE is a collaborative
375 association of state, tribal, and federal agencies, and international partners. U.S. Environmental
376 Protection Agency is the primary funding source, with contracting and research support from the
377 National Park Service. JOK is grateful for access to computing resources provided by the School
378 of Geography and the Environment, University of Oxford. The Air Quality Group at the University
379 of California, Davis is the central analytical laboratory, with ion analysis provided by the Research
380 Triangle Institute, and carbon analysis provided by the Desert Research Institute. We acknowledge
381 the World Climate Research Programme's Working Group on Coupled Modelling, which is
382 responsible for CMIP, and we thank the group of NASA Goddard Institute for Space Studies for
383 producing and making available their GISS-E2-R climate model output. For CMIP the U.S.
384 Department of Energy's Program for Climate Model Diagnosis and Intercomparison provides
385 coordinating support and led development of software infrastructure in partnership with the Global
386 Organization for Earth System Science Portals. The GISS-E2-R dataset were downloaded from
387 <https://cmip.llnl.gov/cmip5/>. We thank the Land-use Harmonization team for producing the
388 harmonized set of land-use scenarios and making available the dataset online at
389 <http://tntcat.iiasa.ac.at/RcpDb/>. We also thank X. Yue for providing the raster of southern
390 California.



391 References

- 392 Abatzoglou, J. T., Kolden, C. A., Balch, J. K., and Bradley, B. A.: Controls on interannual
393 variability in lightning-caused fire activity in the western US, *Environmental Research*
394 *Letters*, 11, 045005, 2016.
- 395 Abatzoglou, J. T., and Williams, A. P.: Impact of anthropogenic climate change on wildfire
396 across western US forests, *Proceedings of the National Academy of Sciences*, 113, 11770-
397 11775, 2016.
- 398 Aerts, R.: The advantages of being evergreen, *Trends in ecology & evolution*, 10, 402-407, 1995.
- 399 Ahlström, A., Schurgers, G., Arneeth, A., and Smith, B.: Robustness and uncertainty in terrestrial
400 ecosystem carbon response to CMIP5 climate change projections, *Environmental Research*
401 *Letters*, 7, 044008, 2012.
- 402 Aitken, S. N., Yeaman, S., Holliday, J. A., Wang, T., and Curtis-McLane, S.: Adaptation,
403 migration or extirpation: climate change outcomes for tree populations, *Evolutionary*
404 *applications*, 1, 95-111, 2008.
- 405 Akagi, S., Yokelson, R. J., Wiedinmyer, C., Alvarado, M., Reid, J., Karl, T., Crouse, J., and
406 Wennberg, P.: Emission factors for open and domestic biomass burning for use in
407 atmospheric models, *Atmospheric Chemistry and Physics*, 11, 4039-4072, 2011.
- 408 Archibald, S., Roy, D. P., van Wilgen, B. W., and Scholes, R. J.: What limits fire? An
409 examination of drivers of burnt area in Southern Africa, *Global Change Biology*, 15, 613-630,
410 2009.
- 411 Balch, J. K., Bradley, B. A., Abatzoglou, J. T., Nagy, R. C., Fusco, E. J., and Mahood, A. L.:
412 Human-started wildfires expand the fire niche across the United States, *Proceedings of the*
413 *National Academy of Sciences*, 114, 2946-2951, 2017.
- 414 Brovkin, V., Boysen, L., Arora, V., Boisier, J., Cadule, P., Chini, L., Claussen, M.,
415 Friedlingstein, P., Gayler, V., and Van Den Hurk, B.: Effect of anthropogenic land-use and
416 land-cover changes on climate and land carbon storage in CMIP5 projections for the twenty-
417 first century, *Journal of Climate*, 26, 6859-6881, 2013.
- 418 Chaste, E., Girardin, M. P., Kaplan, J. O., Portier, J., Bergeron, Y., and Hély, C.: The
419 pyrogeography of eastern boreal Canada from 1901 to 2012 simulated with the LPJ-LMfire
420 model, *Biogeosciences*, 15, 1273-1292, 10.5194/bg-15-1273-2018, 2018.
- 421 Chow, J. C., Watson, J. G., Lowenthal, D. H., Chen, L.-W. A., and Motallebi, N.: PM_{2.5} source
422 profiles for black and organic carbon emission inventories, *Atmospheric Environment*, 45,
423 5407-5414, 2011.
- 424 Ford, B., Val Martin, M., Zelasky, S., Fischer, E., Anenberg, S., Heald, C., and Pierce, J.: Future
425 fire impacts on smoke concentrations, visibility, and health in the contiguous United States,
426 *GeoHealth*, 2, 229-247, 2018.
- 427 Fusco, E. J., Abatzoglou, J. T., Balch, J. K., Finn, J. T., and Bradley, B. A.: Quantifying the
428 human influence on fire ignition across the western USA, *Ecological applications*, 26, 2390-
429 2401, 2016.
- 430 Gelaro, R., McCarty, W., Suárez, M. J., Todling, R., Molod, A., Takacs, L., Randles, C. A.,
431 Darmenov, A., Bosilovich, M. G., and Reichle, R.: The modern-era retrospective analysis for
432 research and applications, version 2 (MERRA-2), *Journal of Climate*, 30, 5419-5454, 2017.
- 433 Giglio, L., Randerson, J. T., and van der Werf, G. R.: Analysis of daily, monthly, and annual
434 burned area using the fourth-generation global fire emissions database (GFED4), *Journal of*
435 *Geophysical Research: Biogeosciences*, 118, 317-328, 2013.



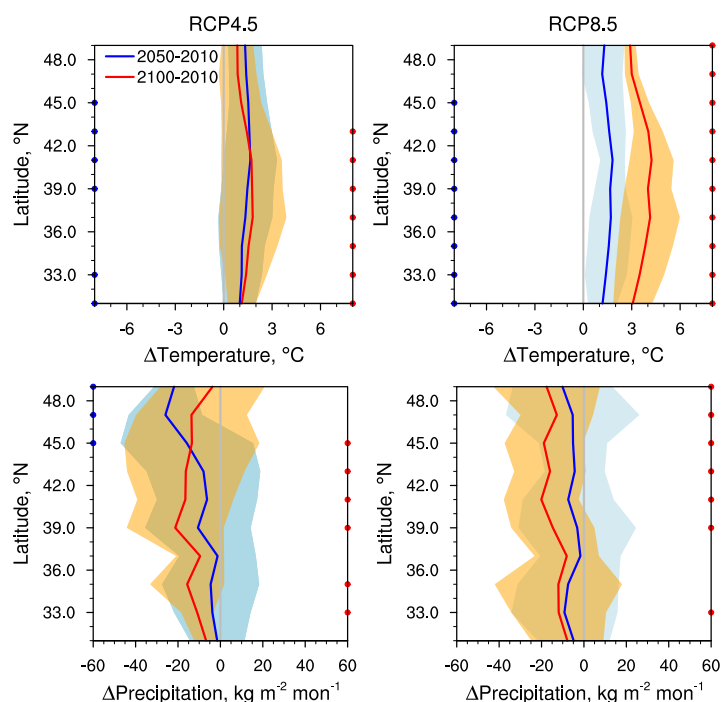
- 436 Jarvis, P., and Leverenz, J.: Productivity of temperate, deciduous and evergreen forests, in:
437 Physiological plant ecology IV, Springer, 233-280, 1983.
- 438 Kumar, S., Dirmeyer, P. A., Merwade, V., DelSole, T., Adams, J. M., and Niyogi, D.: Land
439 use/cover change impacts in CMIP5 climate simulations: A new methodology and 21st
440 century challenges, *Journal of Geophysical Research: Atmospheres*, 118, 6337-6353, 2013.
- 441 Liu, J. C., Wilson, A., Mickley, L. J., Dominici, F., Ebisu, K., Wang, Y., Sulprizio, M. P., Peng,
442 R. D., Yue, X., and Son, J.-Y.: Wildfire-specific Fine Particulate Matter and Risk of Hospital
443 Admissions in Urban and Rural Counties, *Epidemiology (Cambridge, Mass.)*, 28, 77-85,
444 2017.
- 445 Magi, B. I.: Global Lightning Parameterization from CMIP5 Climate Model Output, *Journal of*
446 *Atmospheric and Oceanic Technology*, 32, 434-452, 10.1175/jtech-d-13-00261.1, 2015.
- 447 Nadelhoffer, K. J., Emmett, B. A., Gundersen, P., Kjønaas, O. J., Koopmans, C. J., Schleppei, P.,
448 Tietema, A., and Wright, R. F.: Nitrogen deposition makes a minor contribution to carbon
449 sequestration in temperate forests, *Nature*, 398, 145, 1999.
- 450 Nazarenko, L., Schmidt, G., Miller, R., Tausnev, N., Kelley, M., Ruedy, R., Russell, G., Aleinov,
451 I., Bauer, M., and Bauer, S.: Future climate change under RCP emission scenarios with GISS
452 ModelE2, *Journal of Advances in Modeling Earth Systems*, 7, 244-267, 2015.
- 453 Ortega, A., Day, D., Cubison, M., Brune, W., Bon, D., De Gouw, J., and Jimenez, J.: Secondary
454 organic aerosol formation and primary organic aerosol oxidation from biomass-burning
455 smoke in a flow reactor during FLAME-3, *Atmospheric Chemistry and Physics*, 13, 11551-
456 11571, 2013.
- 457 Park, R. J., Jacob, D. J., Chin, M., and Martin, R. V.: Sources of carbonaceous aerosols over the
458 United States and implications for natural visibility, *Journal of Geophysical Research:*
459 *Atmospheres*, 108, 2003.
- 460 Park, R. J., Jacob, D. J., Field, B. D., Yantosca, R. M., and Chin, M.: Natural and transboundary
461 pollution influences on sulfate-nitrate-ammonium aerosols in the United States: Implications
462 for policy, *Journal of Geophysical Research: Atmospheres*, 109, 2004.
- 463 Pechony, O., and Shindell, D. T.: Driving forces of global wildfires over the past millennium and
464 the forthcoming century, *Proceedings of the National Academy of Sciences*, 107, 19167-
465 19170, 2010.
- 466 Pfeiffer, M., Spessa, A., and Kaplan, J. O.: A model for global biomass burning in preindustrial
467 time: LPJ-LMfire (v1. 0), *Geoscientific Model Development*, 6, 643-685, 2013.
- 468 Price, C., and Rind, D.: Possible implications of global climate change on global lightning
469 distributions and frequencies, *Journal of Geophysical Research: Atmospheres*, 99, 10823-
470 10831, 1994a.
- 471 Price, C., and Rind, D.: The impact of a 2× CO₂ climate on lightning-caused fires, *Journal of*
472 *Climate*, 7, 1484-1494, 1994b.
- 473 Rogers, B. M., Neilson, R. P., Drapek, R., Lenihan, J. M., Wells, J. R., Bachelet, D., and Law, B.
474 E.: Impacts of climate change on fire regimes and carbon stocks of the US Pacific Northwest,
475 *Journal of Geophysical Research: Biogeosciences*, 116, 2011.
- 476 Rupp, D. E., Abatzoglou, J. T., Hegewisch, K. C., and Mote, P. W.: Evaluation of CMIP5 20th
477 century climate simulations for the Pacific Northwest USA, *Journal of Geophysical Research:*
478 *Atmospheres*, 118, 10,884-810,906, 2013.
- 479 Shafer, S. L., Bartlein, P. J., Gray, E. M., and Pelltier, R. T.: Projected Future Vegetation
480 Changes for the Northwest United States and Southwest Canada at a Fine Spatial Resolution



- 481 Using a Dynamic Global Vegetation Model, PLoS One, 10, e0138759,
482 10.1371/journal.pone.0138759, 2015.
- 483 Sheffield, J., Barrett, A. P., Colle, B., Nelun Fernando, D., Fu, R., Geil, K. L., Hu, Q., Kinter, J.,
484 Kumar, S., and Langenbrunner, B.: North American climate in CMIP5 experiments. Part I:
485 Evaluation of historical simulations of continental and regional climatology, Journal of
486 Climate, 26, 9209-9245, 2013.
- 487 Sitch, S., Smith, B., Prentice, I. C., Arneeth, A., Bondeau, A., Cramer, W., Kaplan, J. O., Levis,
488 S., Lucht, W., Sykes, M. T., Thonicke, K., and Venevsky, S.: Evaluation of ecosystem
489 dynamics, plant geography and terrestrial carbon cycling in the LPJ dynamic global
490 vegetation model, Global Change Biology, 9, 161-185, 10.1046/j.1365-2486.2003.00569.x,
491 2003.
- 492 Spracklen, D. V., Mickley, L. J., Logan, J. A., Hudman, R. C., Yevich, R., Flannigan, M. D., and
493 Westerling, A. L.: Impacts of climate change from 2000 to 2050 on wildfire activity and
494 carbonaceous aerosol concentrations in the western United States, Journal of Geophysical
495 Research: Atmospheres, 114, 2009.
- 496 Val Martin, M., Honrath, R., Owen, R. C., Pfister, G., Fialho, P., and Barata, F.: Significant
497 enhancements of nitrogen oxides, black carbon, and ozone in the North Atlantic lower free
498 troposphere resulting from North American boreal wildfires, Journal of Geophysical
499 Research: Atmospheres, 111, 2006.
- 500 Westerling, A., and Bryant, B.: Climate change and wildfire in California, Climatic Change, 87,
501 231-249, 2008.
- 502 Westerling, A. L., Hidalgo, H. G., Cayan, D. R., and Swetnam, T. W.: Warming and earlier
503 spring increase western US forest wildfire activity, science, 313, 940-943, 2006.
- 504 Westerling, A. L.: Increasing western US forest wildfire activity: sensitivity to changes in the
505 timing of spring, Philosophical Transactions of the Royal Society B: Biological Sciences, 371,
506 20150178, 2016.
- 507 Wotton, B., Martell, D., and Logan, K.: Climate change and people-caused forest fire occurrence
508 in Ontario, Climatic Change, 60, 275-295, 2003.
- 509 Yue, X., Mickley, L. J., Logan, J. A., and Kaplan, J. O.: Ensemble projections of wildfire activity
510 and carbonaceous aerosol concentrations over the western United States in the mid-21st
511 century, Atmospheric Environment, 77, 767-780, 2013.
- 512 Yue, X., Mickley, L. J., and Logan, J. A.: Projection of wildfire activity in southern California in
513 the mid-twenty-first century, Climate dynamics, 43, 1973-1991, 2014.
- 514



515 **Figures and tables**

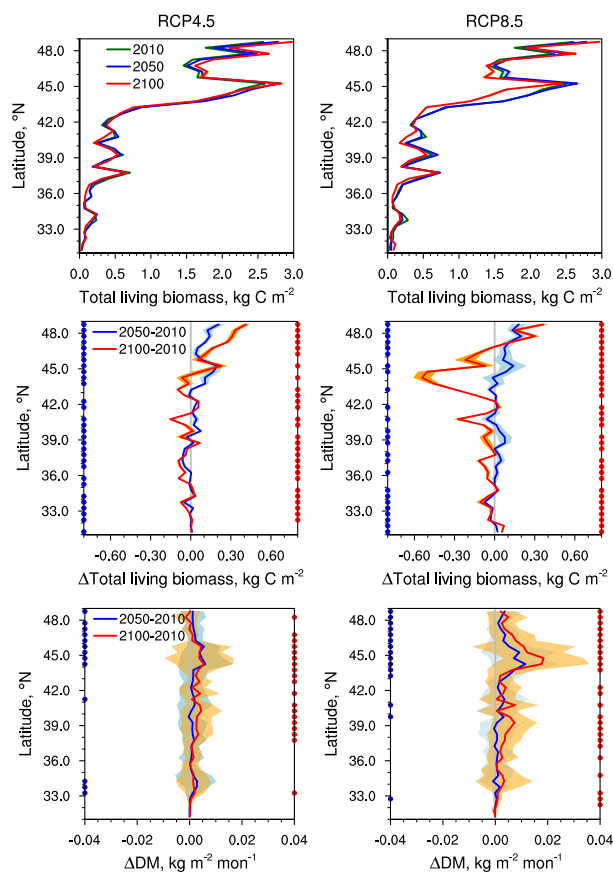


516

517 **Figure 1.** Modeled changes in temperature (top) and precipitation (bottom) in July-August-
518 September (JAS) at ~2050 and ~2100 as a function of latitude over the WUS for RCP4.5 (left)
519 and RCP8.5 (right). Changes are zonally averaged and relative to the present day (~2010), with
520 5-year averages in each time slice. The bold blue lines show the changes between 2010 and
521 2050, averaged over all longitudes in the WUS (31°N – 49°N, 100°W – 125°W); bold red lines
522 show the mean changes between 2010 and 2100. Light blue and orange shadings represent the
523 temporal standard deviation across the 15 months (5 years x 3 months) of each time slice. Blue
524 dots along the axes mark those latitudes showing statistically significant differences between the
525 JAS 2010 and 2050 time slices ($p < 0.05$); red dots mark those latitudes with statistically
526 significant differences at 2100. Temperatures and precipitations are from the GISS-E2-R climate
527 model.



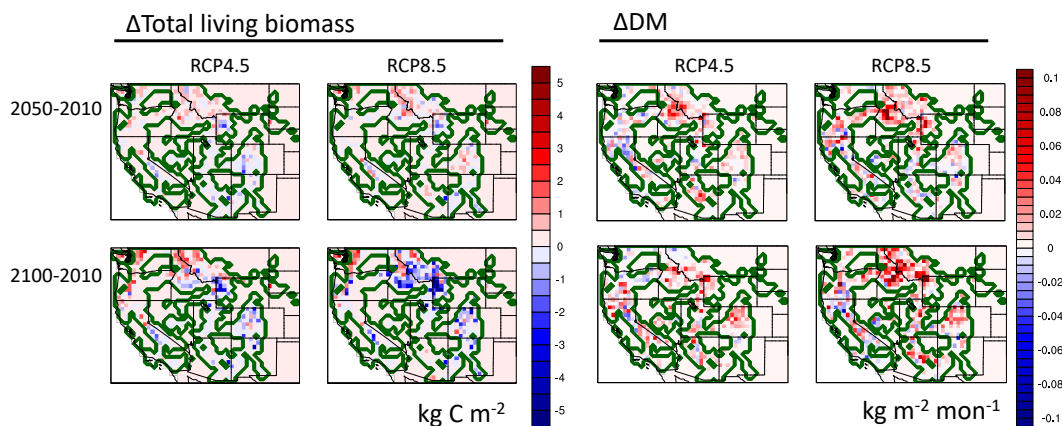
528



529

530 **Figure 2.** The top panel shows total living biomass at ~2010, ~2050 and ~2100 as a function of
531 latitude over the WUS for RCP4.5 (left) and RCP8.5 (right), with 5-year averages in each time
532 slice. The lower four panels are as in Figure 1, but for changes in total living biomass (middle) and
533 lightning-caused dry matter burned (DM; bottom) as a function of latitude over the WUS. Results
534 of living biomass and DM are from LPJ-LMfire. As in Figure 1, dots along the axes mark those
535 latitudes showing statistically significant differences.

536

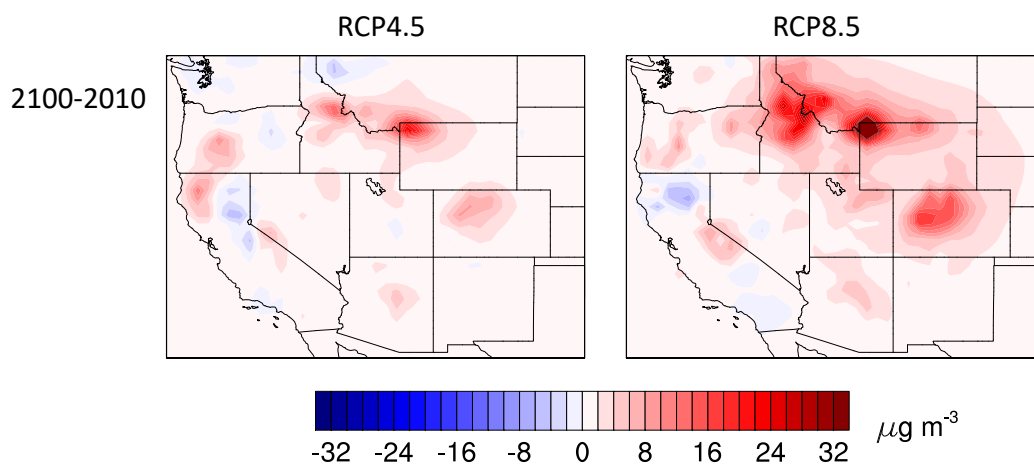


537

538 **Figure 3.** Simulated changes in yearly mean total living biomass and monthly mean DM averaged
539 over the fire season in the National Forests across the WUS for the RCP4.5 and RCP8.5 scenarios.
540 The top row shows changes between the present day and 2050, and the bottom row shows changes
541 between the present day and 2100. Results are from LPJ-LMfire, with five years representing each
542 time period. The fire season is July, August, and September.



543



544

545 **Figure 4.** Simulated changes in fire-season smoke PM (BC+OC) at ~2100 relative to the present
546 day for RCP4.5 and RCP8.5. Results are from GEOS-Chem at a spatial resolution $0.5^\circ \times 0.625^\circ$,
547 averaged over July, August, and September. Each time period is represented by a 5-year time slice.

548



549

Table 1. Total living biomass and dry matter burned (DM) over National Forests and Parks in the WUS and smoke PM (BC+OC) concentrations averaged across the entire West. Also shown is DM summed over National Forests in the Sierra Nevada (SN). Values for the present day (~2010) are shown in the top row; changes in ~2050 and ~2100 relative to the present day are shown in bottom two rows. Statistically significant changes are in boldface.

Time slices	Living biomass ^b , Tg/yr		DM ^b , Tg/JAS		DM in SN ^b , Tg/JAS		BC+OC ^c , $\mu\text{g m}^{-3}$	
	RCP4.5	RCP8.5	RCP4.5	RCP8.5	RCP4.5	RCP8.5	RCP4.5	RCP8.5
2010 ^a	3074.8±33.7	3036.9±55.5	22.16±4.16	30.96±7.15	1.27±1.08	1.24±0.48	2.11±0.48	2.55±0.81
2050-2010 ^a	138.2±46.0	126.2±80.2	18.0±16.1	26.7±14.8	0.22±1.42	0.54±1.50	--	--
2100-2010 ^a	119.6±34.4	-270.7±76.1	24.6±13.2	50.0±18.0	0.91±2.10	1.00±0.86	1.11±1.02	2.78±1.73

^a Each time slice represents 5 years; ^b Values are fire-season summations over National Parks and Forests;

^c BC+OC concentrations are fire-season averages over the West;

Statistical significance is not calculated for living biomass.



550 **Table 2.** Reclassification of LPJ-LMfire PFTs.

LPJ-LMfire (9 pfts)	GEOS-Chem (6 pfts)
Tropical broadleaf evergreen	Tropical forest
Tropical broadleaf raingreen	Tropical forest
Temperate needleleaf evergreen	Temperate forest
Temperate broadleaf evergreen	Temperate forest
Temperate broadleaf summergreen	Temperate forest
Boreal needleleaf evergreen	Boreal forest
Boreal summergreen	Boreal forest
C ₃ grass	Crop, pasture
C ₄ grass	50% -> savanna, grassland, shrubland; 50% -> crop, pasture

551